

Effect of salt on the phase behaviour of F68 triblock PEO/PPO/PEO copolymer

This article has been downloaded from IOPscience. Please scroll down to see the full text article.

2006 J. Phys.: Condens. Matter 18 4461

(<http://iopscience.iop.org/0953-8984/18/19/002>)

View [the table of contents for this issue](#), or go to the [journal homepage](#) for more

Download details:

IP Address: 129.252.86.83

The article was downloaded on 28/05/2010 at 10:39

Please note that [terms and conditions apply](#).

Effect of salt on the phase behaviour of F68 triblock PEO/PPO/PEO copolymer

Y L Wu¹, R Sprik², W C K Poon^{3,4} and E Eiser¹

¹ Department of Chemical Engineering, University of Amsterdam, Nieuwe Achtergracht 166, 1018 WV Amsterdam, The Netherlands

² Van der Waals-Zeeman Instituut, University of Amsterdam, Valckenierstraat 6, 1018 XE Amsterdam, The Netherlands

³ SUPA and School of Physics, The University of Edinburgh, JCMB, The Kings Buildings, Mayfield Road, Edinburgh EH9 3JZ, UK

⁴ FOM Institute for Atomic and Molecular Physics, Kruislaan 407, 1098 SJ Amsterdam, The Netherlands

Received 29 November 2005, in final form 2 March 2006

Published 25 April 2006

Online at stacks.iop.org/JPhysCM/18/4461

Abstract

We studied the effect of sodium chloride on the phase behaviour of the symmetric triblock copolymer F68 in water using direct visual observation, viscometry, small-angle x-ray scattering and microscopy. We found that salt has a destabilizing effect. The transitions from unimer to micellar solution and from micellar solution to BCC micellar crystal occurred some 20 °C lower in 1 M NaCl than in the salt-free system. Salt also induced a region of liquid–liquid coexistence in the phase diagram at F68 concentrations $\lesssim 30$ wt%, with the lower critical solution temperature (or critical point) occurring at ~ 80 °C in 1 M NaCl. At this salt concentration and $\gtrsim 85$ °C, liquid–liquid phase separation becomes metastable. A homogeneous micellar solution at this temperature first separated into coexisting dilute and dense micellar liquids, and then the dense liquid would transform into a transparent ($\lesssim 85$ °C) and turbid ($\gtrsim 85$ °C) mesophase. We tentatively identified these as the BCC cubic and lamellar (L_α) phases respectively. A more complex sequence of observations at a Pluronic concentration of 34 wt% confirms this picture. A phase diagram for F68 in 1 M NaCl consistent with all of our observations is proposed, as well as a ‘rule of thumb’ for interpreting the effect of salt on Pluronic phase behaviour.

(Some figures in this article are in colour only in the electronic version)

1. Introduction

The physics of block copolymer solutions is rich because the *differential solubility* shown by any solvent to the blocks causes self-assembly into various structures. The exact structure formed can be ‘tuned’ by the relative molecular weight of the blocks, the temperature and

polymer concentration, and the solvent composition. Such variety and tunability have led to many applications and an extensive literature [1].

A class of widely used and studied triblock copolymers is formed by a central block of polypropylene oxide (PO) flanked by symmetric blocks of polyethylene oxide (EO), giving the general formula $(EO)_m(PO)_n(EO)_m$ [2]. Individual members of this family, known as Pluronics (or Poloxamers), are labelled Xab . The letter X specifies the room-temperature state ($X = L$ (iquid), P (aste) or F (lake or other solid forms)). The first number a (one or two digits) indicates the molecular weight of the PO block, $M_w^{PO} \approx a \times 300$, while $10 \times b$ gives the approximate wt% of the EO blocks.

The aqueous behaviour of Pluronics is quite distinct from that of a typical small-molecule surfactant. The latter usually micellizes at very low concentrations (ca. 10^{-3} wt%) [3], with the micellization concentration only weakly temperature dependent. However, at low enough temperature (T), both EO and PO are sufficiently soluble for Pluronics to exist in solution as unimers over a range of concentrations (up to $\gtrsim 10$ wt%). As T increases, the decreasing solubility of PO relative to EO results in the formation of spherical micelles at a critical micellization temperature (CMT), which coexist with unimers [4, 5]. These features render aqueous Pluronic solutions robust flocculation and emulsification agents. Micellization of an increasing fraction of the unimers as T is increased further leads to increasing micellar volume fraction and/or changes in micellar shape, which, at high enough copolymer concentration (c), gives rise to various mesophases [1, 2, 6, 7]. Mortensen and co-workers have studied in detail a system, P85, that exemplifies many of these features [2, 7]⁵. On the other hand, Wanka *et al* have obtained the T - c phase diagrams of 20 different Pluronics, and were able to offer some rules of thumb on mesophase formation [6]. They suggest that if the EO:PO ratio $m/n \gtrsim 0.5$, the first mesophase formed upon increasing T or c is the cubic. The hexagonal (H) phase forms first if $m/n \approx 0.25$, while for $m/n \approx 0.15$ the lamellar phase (L_α) forms first.

The effect of various ionic additives on Pluronic behaviour has been the subject of many previous studies [1], partly because of the subject's practical relevance: there are many applications (such as drug delivery) in which the concentrations of various ionic salts and other non-thermal parameters are the preferred means of 'tuning' the properties of Pluronics. As in other soft-matter systems, ion-specific effects beyond simple valence are seen (e.g. [8]). Sodium chloride in general renders Pluronics less soluble. Thus, for example, it lowers the CMT and the 'cloud point' temperature of L64 [8]. The addition of salt can also introduce new mesophases [9, 10]. To date, however, there is no systematic study of how the entire phase diagram of a Pluronic is affected by ionic additives. As a result, and in contrast to the case of changing ' m ' and ' n ', no 'rules of thumb' exist to guide our intuition on the effect of salt on Pluronic phase diagrams.

Below we report how sodium chloride (hereafter simply 'salt') changes the phase diagram of F68, $(EO)_{76}(PO)_{29}(EO)_{76}$. The salt-free phase diagram of F68 is an extremely simple one [6]. The material makes a transition from micellar fluid to a solid cubic phase via a narrow coexistence region as T is increased. The freezing and melting points are strongly decreasing functions of c . Over the range $0^\circ\text{C} < T < 100^\circ\text{C}$ and $0 < c < 100$ wt%, Wanka *et al* observed no other transitions. We found that the addition of sodium chloride complicates this simplicity significantly by making possible transitions other than micelles \rightarrow BCC solid, a result important for the practical 'thermal tuning' of Pluronic solutions. We also observed multi-stepped phase transition kinetics due to the presence of a 'buried' metastable phase boundary. Such kinetics are known in other soft matter systems [11–13], and are important for 'navigating' phase pathways in materials processing. Based on our results, we propose a

⁵ See especially the helpful schematic summary in figure 5 of [2].

simple procedure (the ‘sliding window rule’) for predicting the generic effect of salt on Pluronic phase diagrams.

2. Materials and methods

F68 was purchased from Serva and used without further purification. We prepared samples by dissolving weighed amounts of F68 flakes in water at low temperature. To study the effect of salt, weighed amounts of sodium chloride were added (again at low temperature) after complete dissolution of the F68. Visual observations at different temperatures were carried out by immersing sealed samples in a water bath, where a range of heating rates (from ≈ 0.1 to ≈ 5 °C min⁻¹) could be used. Samples were equilibrated for at least 10 min at each temperature. Optical microscopy was carried out on an inverted Leica DM IRB microscope equipped with a home-built, sealed heating stage.

In a number of cases, we studied the composition of the coexisting phases by measuring their refractive indices and conductivities. These measurements were carried out respectively using an Abbe refractometer from Zeiss to an accuracy of ± 0.001 and on a Cyberscan Con 500 (Eutech Instruments) with a platinum measuring cell of cell constant $k = 10$ cm⁻¹ to an accuracy of ± 0.1 mS.

Viscosity measurements were performed on a stress-controlled Haake RS150 rheometer at a constant stress of 1 Pa in a Couette measuring cell at temperatures between 5 and 60 °C. The dimensions were inner diameter 41.420 mm, outer diameter 43.400 mm, height 55.000 mm and bottom gap 3.000 mm. Samples were loaded at low temperatures where they were in the liquid state, and then heated up *in situ* to the desired temperatures for viscosity determination. Evaporation was kept low by a vapour trap.

Small-angle x-ray scattering (SAXS) measurements were made on the Dutch–Belgium beamline (DUBBLE) BM26 at the ESRF in Grenoble, and the home-built SAXS set-up of W de Jeu (Amolf, the Netherlands). The wavelength used in both instruments was $\lambda = 0.154$ nm. Note that because of the low refractive index and electronic contrast, transition temperatures can only be obtained typically to within ± 2 °C.

3. Results and discussion

3.1. The salt-free system

At low enough T and c , samples were stable indefinitely as homogeneous solutions. Some indication of the nature of the solvated species was obtained from viscosity measurements. The viscosity, η , of a sample at fixed c decreases with increasing T until some temperature T_{\min} , beyond which it increases with T (figure 1(a)). The micellization process in P85 has been studied in detail by Mortensen and co-workers using neutron scattering [14]. Based on the picture they propose, we suggest that the initial decrease of η with T is due to single copolymers (unimers) in solution, whose radius of gyration decreases as water becomes progressively a less good solvent (especially for the PO). We interpret T_{\min} as the CMT. Beyond this point, micelles grow as decreasing solvency drives up the aggregation number; the increasing micellar volume fraction⁶ is reflected in the increase in η .⁷ The CMT of F68 determined this way decreases approximately linearly with c (figure 2). Wanka *et al* have detected the onset of micellization by calorimetry. Their data for PE6800, a Pluronic with composition ($m = 74$, $n = 30$) statistically

⁶ There are some preliminary scattering data for this effect in F68 [15].

⁷ We also detected the onset of micellization using dynamic light scattering, which is not shown here.

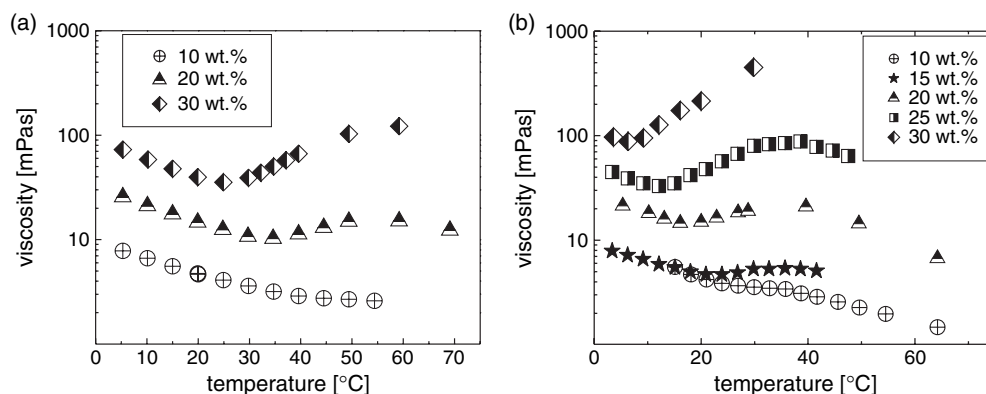


Figure 1. Viscosity data $\eta(T)$ showing the viscosity minimum as T increases. This minimum coincides with the appearance of visible oily streaks. (a) Salt free; (b) 1 M NaCl.

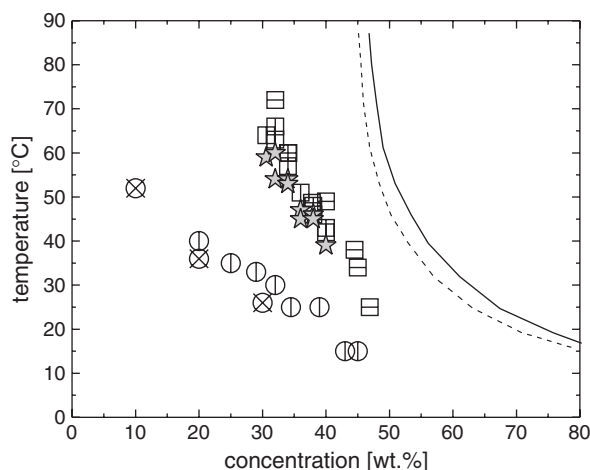


Figure 2. Experimental phase diagram of F68 without added salt. The onset of micellization is obtained from viscosity measurements (crossed circles) and optical observations (other circles). The stars indicate the onset of the two-phase region and the squares the melting line. The lines represent data by Wanka *et al* obtained on a different batch of the F68.

indistinguishable from that of F68 ($m = 76$, $n = 29$), are consistent with what we have found for F68 by viscometry. Upon warming each sample from room temperature, we also noticed the sudden appearance of ‘oily streaks’. The temperature at which this happens as a function of concentration is also shown in figure 1; it is clear that these ‘oily streaks’ are the signature of micellization.

Increasing T or c eventually brought about the onset of liquid–solid coexistence, first observed visually as a ‘ring’ of solid material at the rim of the solution–air interface. Samples at high enough T and c transformed completely into transparent solids. These solids do not yield or flow upon inversion of sample tubes (containing $\approx 1 \text{ cm}^2 \times 4 \text{ cm}$ of material), and remained stable to the highest temperatures investigated ($\geq 90^\circ \text{C}$). The SAXS patterns of these samples displayed Bragg peaks ($q_i/q_0 = 1:\sqrt{3}:\sqrt{4}:\sqrt{5}:\dots$) consistent with a body-centred cubic (BCC) phase [16]. Figure 3 shows the typical phase behaviour observed by SAXS for a

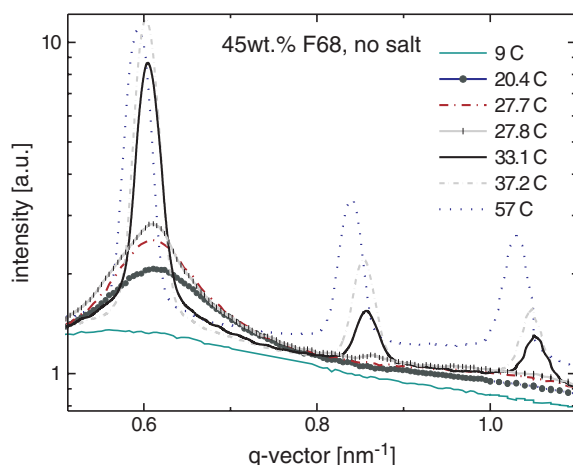


Figure 3. SAXS spectra showing the temperature dependence for a fixed F68 concentration. These spectra were obtained at the DUBBLE beamline/ESRF.

≈ 45 wt% sample. The featureless intensity spectrum at $T = 9^\circ\text{C}$ shows that only unimers are present. Only above 20°C does a broad diffraction ring appear, typical for spherical micelles in solution. The micellar liquid–micellar solid coexistence lies within a small temperature window around $T = 28^\circ\text{C}$, visible as an overlap of a diffuse ring and the onset of sharp Bragg peaks. Finally, above 30°C only sharp Bragg peaks of the BCC crystals are present. Their positions shift slightly towards smaller q -values as the temperature increases, but the BCC signature remains unchanged up to $\approx 90^\circ\text{C}$.

Our phase boundaries, figure 2, have shapes comparable to those reported by Wanka *et al* [6], but have absolute positions displaced to lower T and c ; our coexistence gap is also somewhat wider. These differences are almost certainly attributable to variability in commercial Pluronic [16]. We expect that the physics of these phase boundaries should be qualitatively similar to that already expounded in detail by Mortensen and co-workers [7, 2]: crystallization occurs when the volume fraction of more or less spherical micelles reaches $\gtrsim 50\%$.

3.2. The effect of sodium chloride

We carried out a series of detailed observations and measurements of the phase behaviour of F68 in 1 M sodium chloride.

3.2.1. Micellization and transition to cubic phase. The CMT determined from viscosity measurements, figure 1(b), again decreases approximately linearly with c , figure 4, and with a slope comparable to the salt-free case. But the absolute values have been depressed by $\approx 20^\circ\text{C}$. The phase boundaries for the onset and completion of solidification are also displaced to a similar degree compared to those in the salt-free case. SAXS patterns from the solid were again consistent with a BCC structure.

3.2.2. Cloud point. Heating homogeneous solutions with $c \lesssim 30$ wt% brought the onset of clouding at $T \approx 80^\circ\text{C}$. The turbid samples would subsequently separate into two coexisting clear liquids. (Fluidity was confirmed by tilting the samples and observing the solution–

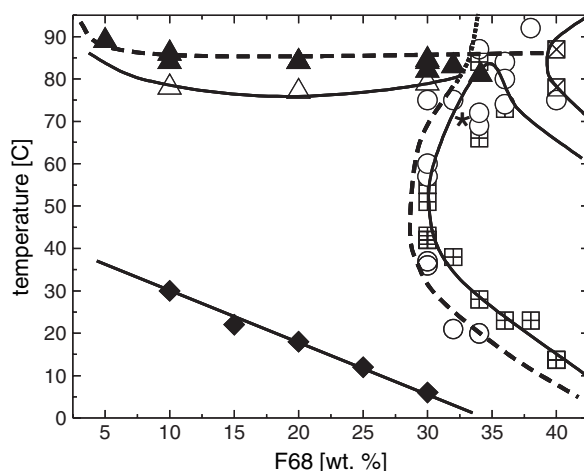


Figure 4. Experimental phase diagram of F68 at 1 M NaCl. The diamonds indicate the CMT. The circles mark the two-phase region between micellar liquid and the BCC or another solid phase. All squares represent regions in which the entire sample was in a single solid phase. The onset of clouding is marked by the open triangles and the solid triangles indicate the temperature at which the initially turbid sample eventually gives rise to liquid-clear solid coexistence. The asterisk marks the two data points (both circles) that do not fit our proposed interpretation. These were probably caused by temperature measurement errors.

solution and solution–air interfaces.) We assume that the coexisting phases brought about by the cloud point transition consist of low and high densities of micelles. The two coexisting solutions remain indefinitely for $T \lesssim 85^\circ\text{C}$. For $T \gtrsim 85^\circ\text{C}$, however, one of the solutions undergoes further transformation after some time (see section 3.2.3).

The locus at which clouding is first observed constitutes the cloud curve, figure 4, with the lowest temperature on it being the lower critical solution temperature (LCST). We find that $\text{LCST} \approx 80^\circ\text{C}$ for F68 in 1 M sodium chloride. Bahadur *et al* have measured the cloud point of a 1 wt% solution of F68 as a function of potassium fluoride concentration [17], extrapolating to $\approx 106 \pm 3^\circ\text{C}$ for the pure Pluronic solution⁸. This suggests that the effect of 1 M salt is to drop the whole cloud curve of F68 by ca. 20°C .

The cloud point transition is associated with the decreasing solubility of the EO ‘corona’ of the Pluronic micelles at high temperatures. Aqueous solutions of polyethylene oxide (PEO) cloud at high temperatures, with the LCST decreasing with molecular weight (M_w). The cloud point of a 1 wt% aqueous solution of PEO with $M_w = 8000$ is $\approx 120^\circ\text{C}$ [18]. The combined molecular weight of the two EO blocks in F68 is $\approx 2 \times 76 \times 44 \approx 7000$, constituting $\approx 80\%$ of the copolymer molecular weight. A cloud point of $\approx 110^\circ\text{C}$ at $c = 1 \text{ wt}\%$ is therefore reasonable.

Salt is known to decrease the solubility of PEO and therefore lowers the cloud point. Thus, for example, 1 M sodium chloride drops the cloud point of a 2.5 mg ml^{-1} ($\approx 0.2 \text{ wt}\%$) solution of PEO with $M_w = 10^6$ by $\approx 30^\circ\text{C}$ [19]. Potassium chloride was found to increase the core radius of F88 micelles [20], while the cloud point of L64 decreases linearly with sodium chloride concentration at a rate of $\approx 20^\circ\text{C M}^{-1}$ [8]. The latter study and the previously quoted data for pure PEO [18] are inconsistent with the 20°C drop in the cloud point we observed in F68 caused by 1 M salt.

⁸ This is from our own analysis of the data in [17]; the authors gave ‘about 105°C ’.

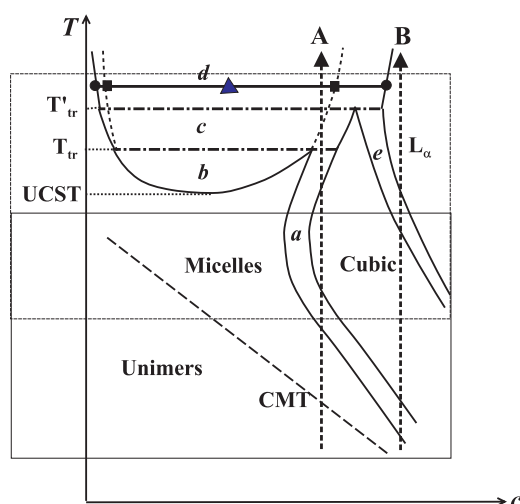


Figure 5. Schematic phase diagram of F68. The dotted and full rectangles are ‘viewing boxes’. The portion within the full rectangle is observed in pure water, while the portion within the dotted rectangle is observed at 1 M salt. Below the dashed line labelled CMT (critical micellization temperature) unimers are the dominant species in solution, while above this line micelles form. Micellar solution and cubic phase coexist in region ‘a’. Above the lower critical solution temperature (LCST), dilute and concentrated micellar solutions coexist in region ‘b’. At the triple temperature T_{tr} , these two micellar solutions coexist with cubic phase, while dilute micellar solution coexists with cubic phase in region ‘c’. At T'_{tr} , dilute micellar solution, cubic and lamellar (L_{α}) phases coexist, while micellar solution and L_{α} coexist in region ‘d’. Coexistence of dense micellar solution and L_{α} obtains in region ‘e’. A homogeneous sample at \blacktriangle will first phase separate into coexisting micellar solutions with compositions given by the two squares, which lie on the metastable extensions of the cloud curve (dashed); subsequently, the system will separate into coexisting micellar solution and lamellar phase with compositions given by the left and right circles respectively. Heating a sample along phase path ‘A’ should transform it from homogeneous solution, via fluid–solid coexistence to fully cubic solid; the latter then melts again and shows solution–cubic phase coexistence without and then with transient L–L coexistence, before finally arriving at solution– L_{α} coexistence. Heating a cubic phase along phase path ‘B’ should transform the sample into cubic– L_{α} coexistence and then fully L_{α} .

3.2.3. Triple points. The high-concentration end of the cloud point curve intersects the low-density branch of the solidification phase boundary at $c \approx 30$ wt% and $T \approx 85$ °C. The latter is the triple temperature, T_{tr} , at which low- and high-density micellar solutions coexist with the cubic phase. Topologically, the phase diagram in the vicinity of T_{tr} has to take the form shown schematically in figure 5. In particular, immediately above T_{tr} , the thermodynamically stable state is the coexistence of low-density micellar solution and cubic phase.

3.2.4. Multi-step kinetics. We have observed the behaviour of a sample with $c = 20$ wt% at $T \gtrsim 80$ °C in detail. At $T < T_{tr} \approx 85$ °C the sample clouded and then separated into coexisting solutions (phases) that remained stable indefinitely. The same initial phenomenology was observed at $T \gtrsim T_{tr}$, but now the liquid–liquid coexistence was only metastable: after some time, the lower (more concentrated) phase transformed into a clear solid. SAXS patterns of this solid were consistent with a BCC structure.

We determined the refractive index and conductivity of the transient coexisting liquid phases for three samples. The results are shown in table 1. First note that the conductivities of the upper and lower phases are, within experimental error, constant at ≈ 80 and ≈ 20 mS

Table 1. The refractive index (n) and conductivity (σ) of the transient coexisting upper and lower liquid phases in three samples with different average F68 concentrations ([F68]).

[F68] (wt%)	Phase	Phase fraction (%)	n	σ (mS)
15	Upper	59	1.346	80.1
	Lower	41	1.383	19.0
20	Upper	45	1.347	81.4
	Lower	55	1.384	19.4
25	Upper	32	1.348	82.4
	Lower	68	1.387	19.6

respectively, implying a fixed salt concentration in these phases. Next we note that the refractive indices of the coexisting upper and lower phases are also constant across the three samples: ≈ 1.35 and ≈ 1.38 respectively. Thus, at fixed temperature, as we changed the composition of the samples, the coexisting phases remained constant in composition, although the relative amounts of the phases changed. These observations are consistent with these samples lying on a single tie line within a ‘buried’, metastable continuation of the cloud curve within the micellar–cubic and micellar–lamellar coexistence regions (figure 5).

We also observed the sample with $c = 20$ wt% in an optical microscope at $\approx T_{tr}$. Since the temperature controller had finite precision, the temperature of the sample slowly oscillated from just above, T_{tr}^+ , to just below, T_{tr}^- , this value. At T_{tr}^- we observed round droplets that were mobile and, when they touched, coalesced. Once the temperature rose to T_{tr}^+ , however, all droplet motion and coalescence ceased. These observations are consistent with droplets of dilute micellar solution moving and coalescing in a background of dense micellar solution at T_{tr}^- , which become immobilized as the background turns into solid cubic phase at T_{tr}^+ .

Next, we took this sample, equilibrated it at 85°C (i.e. let it successively go from liquid–liquid to liquid–BCC solid coexistence), and then heated it to $\gtrsim 90^\circ\text{C}$. The clear solid turned translucent. This new solid phase is soft—rigorous shaking of the tube led to its yielding and flow. On the other hand, if we heated the same sample in its micellar phase at room temperature rapidly to $T \gtrsim 90^\circ\text{C}$ directly (without equilibrating at 85°C), it again first clouded and separated into two solutions. The translucent solid subsequently developed out of the lower (more concentrated) solution. It was unclear whether the latter process occurred *via* a clear–solid intermediate.

We propose that the translucent solid is a lamellar, or L_α , phase. Compared to the cubic phase, the soft lamellae both fluctuate more (and hence scatter light more strongly) and yield at much lower stresses [21]. If this proposal is correct, then there exists a further triple temperature, $T_{tr}' \approx 90^\circ\text{C}$, at which dilute micellar solution coexists with two mesophases: BCC crystals and L_α lamellae, figure 5.

3.2.5. Other observations. If indeed two triple points exist in F68 in 1 M sodium chloride associated with cubic and lamellar mesophases, then thermodynamic theory dictates the phase diagram topology sketched schematically in figure 5. A detailed set of observations for a sample with $c = 30$ wt% and less detailed observations for samples at higher concentrations confirm this topology, and provide some insight into the precise geometry of the phase boundaries in this high-concentration regime.

A sample with $c = 30$ wt% was a homogeneous solution just below room temperature. Solution–clear solid coexistence was first observed at $T \approx 20^\circ\text{C}$, with complete solidification at $T \approx 40^\circ\text{C}$. Thereafter, the sample remained a clear solid until just below 60°C , whereupon partial melting into a clear liquid started. Thereafter, there was a window of temperatures in

which the sample appeared to be in liquid–clear solid coexistence again, before cloudiness was observed. Reference to figure 5 shows that this sequence of observations is consistent with the behaviour of a sample along phase path ‘A’.

Other observations of samples with $c > 30$ wt% are summarized in figure 4. In particular, a sample with $c = 40$ wt% was a clear solid at room temperature, and remained so until $T \gtrsim 70$ °C. Further heating brought about the onset of cloudiness, until at $T \gtrsim 80$ °C, the sample was a fully translucent solid. Reference to figure 5 shows that these observations are consistent with the behaviour of a sample along phase path ‘B’.

Phase boundaries consistent with all our observations and reflecting the topology shown in figure 5 are sketched out in figure 4. Only two samples (marked with an asterisk) do not fit into this interpretive scheme; these were probably due to errors in temperature measurement. We also made limited observations at other salt concentrations up to 2 M. In all cases, the relevant properties appear to scale more or less linearly with salt concentration in this range.

4. Summary and conclusions

We found that 1 M sodium chloride drops the CMT, the micelle–cubic phase coexistence region, and the cloud curve of F68 by ~ 20 °C, and exposes two triple points associated with cubic and lamellar mesophases. A convenient way to summarize these observations is to say that the effect of salt is to move an ‘observation window’ upwards in a ‘master phase diagram’, figure 5, with a concomitant rescaling of the temperature axis. It would be interesting to test the applicability of this simple ‘sliding window’ to understanding the effect of salt on the phase behaviour of other Pluronics. It is probable that, in the general case, the ‘sliding window’ rule has to be supplemented with a change in effective EO to PO ratio, as salt affects the solubility of the PO block more strongly than the EO block.

At and above the first triple temperature, T_{tr} (figure 5), we found various multi-stepped kinetics. These are examples of a thermodynamic system exploiting a metastable minimum in its ‘free energy landscape’ (here the metastable minimum is associated with the dense micellar solution) to reach equilibrium in two steps—this route being kinetically less costly than the alternative, single-stepped route [11, 22]. Here, for example, heating an initially fluid 20 wt% sample can transform part of it into lamellar phase via metastable demixing into dilute and dense micellar solutions; this is kinetically easier than converting a denser (≈ 40 wt%) sample fully into lamellar phase by heating, because this route goes via an equilibrium cubic phase. The physics of such multi-stepped kinetics on complex free-energy landscapes [22] has been studied before in colloid–polymer mixtures [12] and in surfactant solutions [13].

Acknowledgments

We thank Liddy van der Burg for technical help throughout this work, and Professor Stefan Egelhaaf for helpful discussions. We also thank Professor W de Jeu for making his SAXS equipment at the FOM institute (NL) available, and Dr D Byelov for assistance. WCKP was partly funded by a Joop Los Fellowship at the FOM institute.

References

- [1] Hamley I W 1998 *Physics of Block Copolymers* (Oxford: Oxford University Press)
- [2] Mortensen K 2001 *Colloids Surf.* **183–185** 277
- [3] Israelachvili J 1991 *Intermolecular and Surface Forces* (New York: Academic)
- [4] Linse P 1993 *Macromolecules* **26** 4437

-
- [5] Wijmans C M, Eiser E and Frenkel D 2004 *J. Chem. Phys.* **120** 5839
 - [6] Wanka G, Hoffmann H and Ulbricht W 1994 *Macromolecules* **27** 4145
 - [7] Mortensen K 1996 *J. Phys.: Condens. Matter* **8** A103
 - [8] Alexandridis P and Holzwarth J F 1997 *Langmuir* **13** 6074
 - [9] Jørgensen E B and Hvidt S 1997 *Macromolecules* **30** 2355
 - [10] Thiyagarajan P and Fan L 2002 *Appl. Phys. A* **74** S525
 - [11] Evans R M, Renth F and Poon W C K 2001 *Phys. Rev. E* **64** 031402
 - [12] Renth F, Evans R M and Poon W C K 2001 *Phys. Rev. E* **64** 031403
 - [13] Buchanan M, Starrs L, Egelhaaf S U and Cates M E 2000 *Phys. Rev. E* **62** 6895
 - [14] Mortensen K and Pedersen J S 1993 *Macromolecules* **26** 805
 - [15] Borbély S 1998 *Physica A* **243** 1016
 - [16] Eiser E, Molino F, Porte G and Diat O *Phys. Rev. E* **61** 6759
 - [17] Bahadur P, Li P, Almgren W and Brown W 1992 *Langmuir* **8** 1903
 - [18] Saeki S, Kuwahara N, Nakata M and Kaneko M 1976 *Polymer* **17** 685
 - [19] Armstrong J K, Leharne S A, Stuart B H, Snowden M J and Chowdhry B Z 2001 *Langmuir* **17** 4482
 - [20] Jain N J, Aswal V K, Goyal P S and Bahadur P 1998 *Langmuir* **10** 8452
 - [21] Ramos L and Porte G, private communication
 - [22] Poon W C K, Renth F and Evans R M 2000 *J. Phys.: Condens. Matter* **12** A269